POWER ELECTRONICS AND DRIVES
2(37), No. 2, 2017 DOI: 10.5277/PED170205

STATE OBSERVER FOR DOUBLY-FED INDUCTION GENERATOR

KRZYSZTOF BLECHARZ, DANIEL WACHOWIAK, ZBIGNIEW KRZEMIŃSKI

Gdansk University of Technology
E-mail addresses: krzysztof.blecharz@pg.edu.pl, daniel.wachowiak@pg.edu.pl, zbigniew.krzeminski@pg.edu.pl

Abstract: The purpose of this paper is to show a new state observer for doubly-fed generator. A proposed *z*-type observer algorithm based on mathematical model of doubly fed generator with additional variables treated as a disturbances has been used. A nonlinear multiscalar control method has been proposed to control active and reactive power of the generator. All analyses were verified by simulations and experiments tests.

Keywords: *doubly-fed induction generator, non-linear control, state observer, power control*

1. INTRODUCTION

A doubly fed induction generator (DFIG) is a very popular solution in modern high power wind turbines due to its properties. This kind of generator is characterized by some key features such as good dynamic properties, wide range of speed changes, independent active and reactive power control.

In DFIG power control algorithms, rotor position and speed are required to transform state variables between different coordinate systems. The simplest solution is to use a mechanical encoder but this approach is expensive and requires additional signal cable. There is a tendency, especially in the case of high power generator systems, to eliminate the speed sensor to improve overall system reliability. Replacing the mechanical sensor with a speed estimation algorithm provides other benefits like additional diagnostic information. The problem of rotor speed and position estimation has been widely discussed [1–4].The most common and simple approach is to calculate the rotor current in the stationary reference frame oriented with stator and compare the results with a measured value in the stationary rotor reference frame. These calculations are based on a stator flux equations, therefore are sensitive to stator voltage fluctuations. Another form of rotor angle and speed estimation are various variants of model

Manuscript received: October 4, 2017; accepted: November 15, 2017.

reference adaptive system (MRAS) observers [5, 6], but these algorithms are sensitive to generator parameters errors.

In this paper a novel sensorless nonlinear control algorithm has been proposed to control a doubly-fed induction generator. The nonlinear multiscalar control of active and reactive power and the new speed observer for DFIG can be interesting alternative to classic field oriented control and direct power control methods. The presented observer may be useful for a diagnostics system in some wind power plants [7].

2. MULTISCALAR MODEL OF DFIG

To ensure independent control of active and reactive power of DFIG, a nonlinear control method was used. Variation of nonlinear control method based on the multiscalar *z*-type model of a wound rotor induction machine has been used. To create a multiscalar *z*-type model of the generator, it is necessary to adopt new variables defined as scalar and vector product of stator flux $\boldsymbol{\Psi}_s$ and rotor current vectors $\mathbf{i}_r$. It is possible to take different pairs of vectors. The new variables for multiscalar *z*-type model are defined as follows:

$$z_{11} = \omega_r \tag{1}$$

$$z_{12} = \psi_{s\alpha} i_{r\beta} - \psi_{s\beta} i_{r\alpha} \tag{2}$$

$$z_{21} = \psi_s^2 \tag{3}$$

$$z_{22} = \psi_{s\alpha} i_{r\alpha} + \psi_{s\beta} i_{r\beta} \tag{4}$$

Differentiation of the multiscalar variables defined above and using a vector model of a generator leads to the system of differential equations that describe dynamics of the machine. This system of four equations is called the multiscalar *z*-type model of DFIG [8]. A detailed synthesis procedure of nonlinear power control structure based on multiscalar *z*-type model of a DFIG has been described in [8]. All differential equations are nonlinear and therefore input-output linearization method was used. The decoupling equations have the following form:

$$u_{r1} = \frac{1}{a_{24}} \left(-z_{11}(z_{22} + a_{22} z_{21}) + a_{22} u_{sf1} - u_{si1} - \left(a_{11} + a_{21} \right) m_1 \right) \tag{5}$$

$$u_{r2} = \frac{1}{a_{24}} \left(-a_{23} z_{21} - a_{12} i_r^2 + z_{11} z_{12} + a_{22} u_{sf2} - u_{si2} - \left(a_{11} + a_{21} \right) m_2 \right) \tag{6}$$

where,

$$u_{sf1} = u_{s\beta}\psi_{s\alpha} - u_{s\alpha}\psi_{s\beta} \tag{7}$$

$$u_{sf2} = u_{s\alpha}\psi_{s\alpha} + u_{s\beta}\psi_{s\beta} \tag{8}$$

$$u_{si1} = u_{s\alpha}i_{r\beta} - u_{s\beta}i_{r\alpha} \tag{9}$$

$$u_{si2} = u_{s\alpha}i_{r\alpha} + u_{s\beta}i_{r\beta} \tag{10}$$

are additional auxiliary variables and a_{11}, a_{22}, a_{21}, a_{23}, a_{24} are functions of generator parameters and are defined as $a_{11} = -R_s/L_s$, $a_{12} = R_sL_m/L_s$, $a_{21} = -(L_s^2R_r + R_sL_m^2)/(L_sw_\sigma)$, $a_{22} = L_m/w_\sigma$, $a_{23} = R_sL_m/(L_sw_\sigma)$, $a_{24} = L_s/w_\sigma$, $w_\sigma = L_sL_r - L_m^2$. Variables m_1 and m_2 are new control signals. The components of the rotor voltage vector may be calculated from the values of u_{r1} and u_{r2} variables by using the expressions:

$$u_{r\alpha S} = \frac{u_{r1}\psi_{s\beta} + u_{r2}\psi_{s\alpha}}{z_{21}} \tag{11}$$

$$u_{r\beta S} = \frac{u_{r2}\psi_{s\beta} - u_{r1}\psi_{s\alpha}}{z_{21}} \tag{12}$$

The active and reactive power of the generator can be expressed by the multiscalar variables in per unit as follows:

$$P_S = \frac{1}{L_s}u_{sf2} - \frac{L_m}{L_s}\frac{u_{sf1}z_{12} + u_{sf2}z_{22}}{z_{21}} \tag{13}$$

$$Q_S = \frac{1}{L_s}u_{sf1} - \frac{L_m}{L_s}\frac{u_{sf1}z_{22} - u_{sf2}z_{12}}{z_{21}} \tag{14}$$

To control the generator powers at stator side, accordingly with the equations (13) and (14), it is necessary to force the values of z_{12} and z_{22} variables. It should be noted that the equations (13), (14) may by simplified due to the fact that in steady-state the auxiliary variables u_{sf1} and u_{sf2} are approximately equal to 1 and 0 in pu.

The DFIG power control structure shown in Fig. 1 contains two cascade control loops. The outer loop controls both the stator active and reactive power according to values received from the different higher level control algorithm of powers. On the other hand, the inner control loop task consists of independent control of the z_{12} and z_{22} multiscalar variables. PI controllers were used in both control loops. For the calculation of multiscalar variables, an information about rotor currents and stator flux is needed. In this kind of generator, the rotor currents are measurably available but the stator flux has to be estimated. In an original version of the control system, the stator flux was calculated

by integrating the stator voltage, including the voltage drop across the stator resistance. This approach to estimation of the stator flux requires elimination of constant components of voltage and current measurements. In the proposed control structure, a new state observer, described in next section, was used.

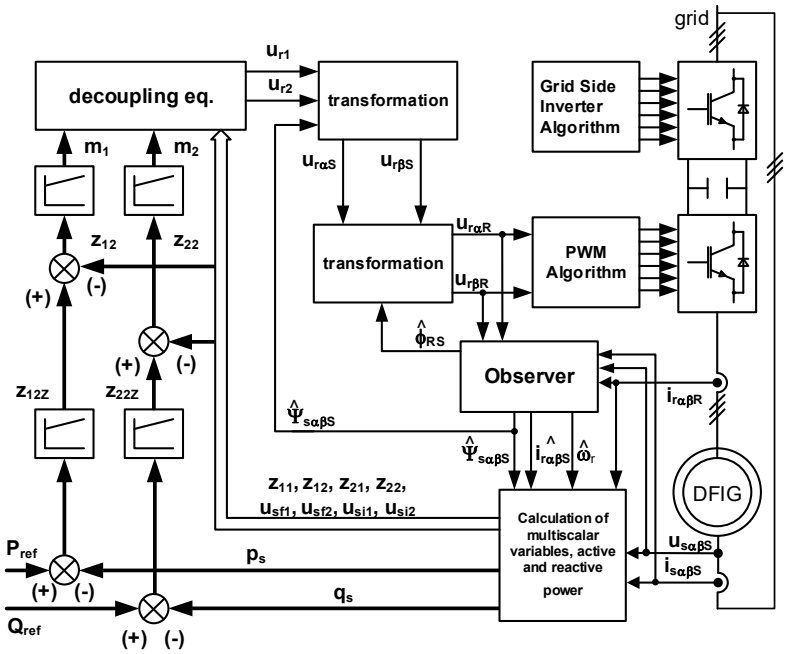

Fig. 1. Schematic diagram of the proposed power control system

3. STATE OBSERVER FOR DFIG

3.1. MATHEMATICAL MODEL OF THE STATE OBSERVER

The structure of analyzed state observer was presented for the first time in [9]. The structure of the observer is based on mathematical model of the induction machine and Luenberger observer theory. In the equations of the speed observer, the components of the electromotive force vector were defined as additional state variables treated as disturbance. The electromotive forces, denoted by ζ, are represented by

$$\zeta = \omega_r \psi_s \tag{15}$$

where ω_r is the rotor speed of the machine. If the stator flux $\mathbf{\Psi}_s$ and the rotor current $\mathbf{i}_r$ space vectors are chosen as state observer equations in simple vector form are defined as follows

$$\frac{d\hat{\boldsymbol{\psi}}_s}{d\tau} = a_{11}\hat{\boldsymbol{\psi}}_s + a_{12}\hat{\mathbf{i}}_r + \mathbf{u}_s + k_2 j\tilde{\boldsymbol{\zeta}} \tag{16}$$

$$\frac{d\hat{\mathbf{i}}_r}{d\tau} = a_{21}\hat{\mathbf{i}}_r - ja_{22}\boldsymbol{\zeta} + a_{23}\hat{\psi}_s - a_{22}\mathbf{u}_s + a_{24}\mathbf{u}_r + k_3\tilde{\mathbf{i}}_r \tag{17}$$

$$\frac{d\boldsymbol{\zeta}}{d\tau} = a_{11}\hat{\omega}_r\hat{\boldsymbol{\psi}}_s + a_{12}\hat{\omega}_r\hat{\mathbf{i}}_\mathbf{r} + \hat{\omega}_r\mathbf{u}_\mathbf{s} - jk_1\tilde{\mathbf{i}}_\mathbf{r} \tag{18}$$

where, k_1, k_2, k_3 are gains of the state observer , a_{11}, a_{22}, a_{21}, a_{23}, a_{24} are functions of generator parameters and are defined similarly to multiscalar *z*-type model.

It was assumed that machine parameters used in the speed observer are known and have been designated by a different algorithm. All estimated variables are denoted by the symbol ^. The measured and controlled rotor current and electromotive force were selected as a corrective feedback to the speed observer. The correcting errors are denoted by the symbol ~ and defined as:

$$\tilde{\mathbf{i}}_r = \mathbf{i}_r - \hat{\mathbf{i}}_r \tag{19}$$

$$\tilde{\boldsymbol{\zeta}} = \hat{\omega}_r\hat{\boldsymbol{\Psi}}_s - \boldsymbol{\zeta} \tag{20}$$

The estimated speed can be expressed by the following equation

$$\hat{\omega}_r = \frac{\zeta_\alpha\hat{\psi}_{s\alpha} + \zeta_\beta\hat{\psi}_{s\beta}}{\hat{\psi}_s{}^2} \tag{21}$$

3.2. STABILITY ANALYSIS AND GAINS

The basic requirement of sensorless drives is to provide stability of the speed observer. According to the first Lyapunov method, an equilibrium point of a system is stable if the linearized system is stable. Stability of the observer can be ensured by proper gains selection to place all poles of the state matrix of the linearized system on the left side of the complex plane. The equations describing dynamics of errors of the extended speed observer are defined by (22)–(26). The first two differential equations are the result of subtracting the observer equations from the model equations. It is not possible to express the estimated rotor speed or rotor speed error with variable $\tilde{\zeta}$ error instead of calculated variable ζ, therefore the equation (24) describes rather dynamics of variable ζ than error of variable $\tilde{\zeta}$.

$$\frac{d\tilde{\boldsymbol{\Psi}}_s}{d\tau} = \left(a_{11} + jk_2\hat{\omega}_r\right)\tilde{\boldsymbol{\Psi}}_s + a_{12}\tilde{\mathbf{i}}_r - jk_2\left(\hat{\omega}_r\boldsymbol{\Psi}_s - \boldsymbol{\zeta}\right) \tag{22}$$

$$\frac{d\tilde{\mathbf{i}}_r}{d\tau} = \left(a_{21} - k_3 + j\hat{\omega}_r\right)\tilde{\mathbf{i}}_r + j\tilde{\omega}_r\mathbf{i}_r + ja_{22}\left(\omega_r\boldsymbol{\Psi}_s - \boldsymbol{\zeta}\right) + a_{23}\tilde{\boldsymbol{\Psi}}_s \tag{23}$$

$$\frac{d\boldsymbol{\zeta}}{d\tau} = a_{11}\hat{\omega}_r\boldsymbol{\Psi}_s - a_{11}\hat{\omega}_r\tilde{\boldsymbol{\Psi}}_s + a_{12}\hat{\omega}_r\mathbf{i}_r - a_{12}\hat{\omega}_r\tilde{\mathbf{i}}_r + \hat{\omega}_r\mathbf{u}_s - jk_1\tilde{\mathbf{i}}_r \tag{24}$$

$$\hat{\omega}_r = \frac{\zeta_\alpha\left(\psi_{s\alpha} - \tilde{\psi}_{s\alpha}\right) + \zeta_y\left(\psi_{s\beta} - \tilde{\psi}_{s\beta}\right)}{\left(\psi_{s\alpha} - \tilde{\psi}_{s\alpha}\right)^2 + \left(\psi_{s\beta} - \tilde{\psi}_{s\beta}\right)^2} \tag{25}$$

$$\tilde{\omega}_r = \omega_r - \frac{\zeta_\alpha\left(\psi_{s\alpha} - \tilde{\psi}_{s\alpha}\right) + \zeta_\beta\left(\psi_{s\beta} - \tilde{\psi}_{s\beta}\right)}{\left(\psi_{s\alpha} - \tilde{\psi}_{s\alpha}\right)^2 + \left(\psi_{s\beta} - \tilde{\psi}_{s\beta}\right)^2} \tag{26}$$

In the steady state of the observer, zero estimation errors are expected. The operating point of the observer are zeros of the rotor current and stator flux estimation errors. According to the definition (15), in the steady state it is also expected that variable ζ of the observer is equal to the product of the rotor speed and stator flux. The operating point of the observer $\overline{\mathbf{x}}$ is defined as (27). Such operating point is also an equilibrium of dynamic system (22)–(24).

$$\overline{\mathbf{x}} = \left[\tilde{\mathbf{i}}_r \quad \overline{\tilde{\boldsymbol{\Psi}}}_s \quad \overline{\boldsymbol{\zeta}}\right]^T = \left[0 \quad 0 \quad \omega_r\boldsymbol{\Psi}_s\right]^T \tag{27}$$

The result of the linearization is in the form of

$$\frac{d\Delta\mathbf{x}}{d\tau} = \mathbf{A}\Delta\mathbf{x} \tag{28}$$

where $\Delta\mathbf{x}$ is a vector of deviations from the operating point. The matrix $\mathbf{A}$ is the Jacobian of dynamic system (22)–(27) at an equilibrium $\overline{\mathbf{x}}$.

$$\Delta\mathbf{x} = \left[\tilde{\mathbf{i}}_r - \overline{\tilde{\mathbf{i}}}_r \quad \tilde{\boldsymbol{\Psi}}_s - \overline{\tilde{\boldsymbol{\Psi}}}_s \quad \boldsymbol{\zeta} - \overline{\boldsymbol{\zeta}}\right]^T = \left[\tilde{\mathbf{i}}_r \quad \tilde{\boldsymbol{\Psi}}_s \quad \Delta\boldsymbol{\zeta}\right]^T \tag{29}$$

$$\Delta\boldsymbol{\zeta} = \boldsymbol{\zeta} - \hat{\omega}_r\hat{\boldsymbol{\Psi}}_s \tag{30}$$

$$\mathbf{A}=\begin{bmatrix} a_{11} & \omega_a-k_2\omega_r & a_{12} & 0 & 0 & -k_2 \\ -\omega_a & a_{11} & 0 & a_{12} & 0 & 0 \\ a_{23} & 0 & a_{21}-k_3 & \omega_a-\omega_r & 0 & a_{22} \\ 0 & a_{23} & -(\omega_a-\omega_r) & a_{21}-k_3 & -a_{22} & 0 \\ \left(a_{12}\omega_r\dfrac{i_{rd}}{\psi_{sd}}+\omega_r\dfrac{u_{sd}}{\psi_{sd}}\right) & 0 & -a_{12}\omega_r & k_1 & \left(a_{11}+a_{12}\dfrac{i_{rd}}{\psi_{sd}}+\dfrac{u_{sd}}{\psi_{sd}}\right) & \omega_a \\ \left(a_{12}\omega_r\dfrac{i_{rq}}{\psi_{sd}}+\omega_r\dfrac{u_{sq}}{\psi_{sd}}\right) & -a_{11}\omega_r & -k_1 & -a_{12}\omega_r & \left(a_{12}\dfrac{i_{rq}}{\psi_{sd}}+\dfrac{u_{sq}}{\psi_{sd}}-\omega_a\right) & 0 \end{bmatrix} \tag{31}$$

The values λ_1, ..., λ_6 satisfying equation (32) will be called observer poles in this paper. The elements of the matrix **A** depend not only on constant values like coefficients a_{11} or a_{22}, etc., which depend on motor parameters, or observer gains k_1–k_3 but also on variable values like rotor speed or components of rotor current and stator flux vectors. The rotor speed is a slow-paced variable and in the steady state can be considered as constant. Vector components expressed in the stator reference frame, on the other hand, change sinusoidal in time what makes poles placement analysis impossible. Therefore linearized equations are represented in the stator flux reference frame

$$\left|\mathbf{A}-\mathbf{I}\lambda\right|=0 \tag{32}$$

The matrix **A** depends on observer gains, therefore the gains have influence on the observer dynamics and stability. Poles placement depends also on the rotor speed, the module of stator flux vector and components of rotor current vector. The module of stator flux vector is kept at a constant level by a control algorithm. The rotor current components are influenced by active and reactive power of the plant. Simulation experiments confirmed that changes of plant power do not have any significant influence on poles placement. It emerges that the only variable affecting observers dynamics is rotor speed. Poles placement in function of rotor speed is presented in Figs. 2 and 3. Two sets of values of stator active and reactive power are investigated. In the first case, the values of active power and reactive power were $s_p = -0.3$, and $s_q = -0.5$, respectively (lagging power factor). In the second case, active and reactive power ware $s_p = -0.4$, and $s_q = 0.4$ (leading power factor). In both scenarios, acquired poles placements are comparable, thus similar dynamic properties are expected regardless of active or reactive power of the machine.

All poles of the observer are placed in the left half-plane for all examined values of the rotor speed what ensures the stability of the observer. The observer poles are calculated on a basis of the linearized system so conclusions about its dynamic properties drawn from eigenvalues of the matrix **A** are valid only in states which are close to the operating point. This means that the stability of the observer is not guaranteed if estimations

errors are big. However, simulation experiments verify that even when the observer starts with initial errors exceeding 100%, it is able to converge towards zero errors.

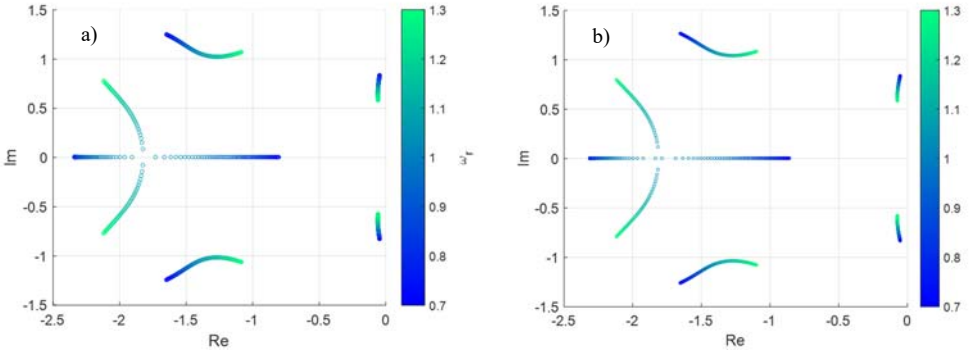

Fig. 2. Poles placement of the speed observer in function of rotor speed presented on the complex planes for various values of active and reactive power: a) $\Psi_r = 0.95$, $s_p = -0.3$, $s_q = -0.5$ b) $\Psi_r = 0.95$, $s_p = -0.3$, $s_q = 0.4$

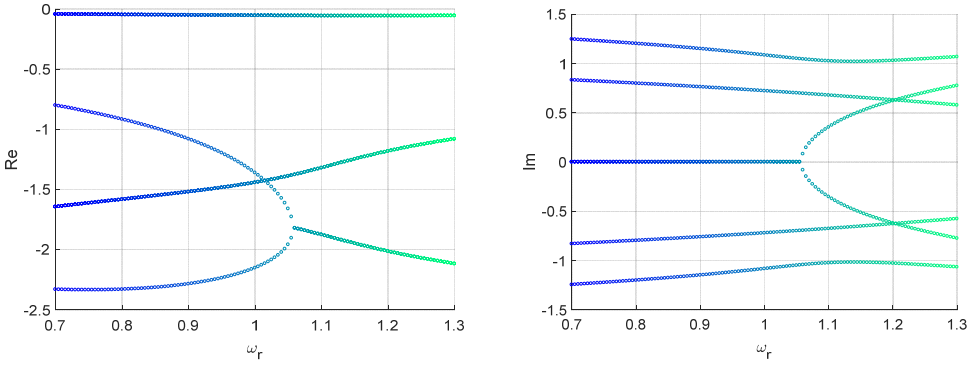

Fig. 3. Real (left) and imaginary (right) part of speed observer poles in function of rotor speed for $\Psi_r = 0.95$, $s_p = -0.3$, $s_q = -0.5$

The dynamic properties of the speed observer are determined mainly by dominant poles, which are poles placed closest to the imaginary axis. Influence of deviations from the observer gains on the placement of the dominant poles is shown in Fig. 4. Deviations of ±10% of the original values of k_1, k_2 and k_3 are investigated. In all cases, poles remain on the left side of the complex plane what insures stability of the observer. It can be noticed that lower values of the observer gains (Fig. 4a) cause dominant poles to be placed closer to the imaginary axis what affects observer dynamics. Increasing the gains (Fig. 4h) moves the dominant poles away from the imaginary axis improving observer dynamics. It is, though, not advisable to assign too high observer gains as they may amplify current measurement noise and errors.

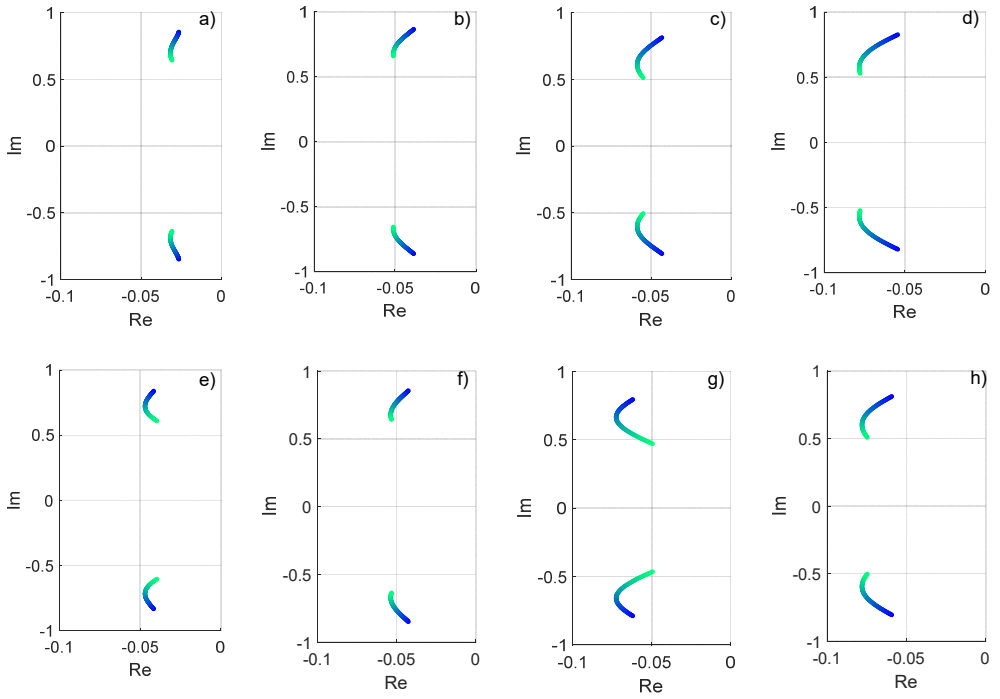

Fig. 4. Placement of the dominant poles of the speed observer in function of the rotor speed; $\psi_r = 0.95$, $s_p = -0.3$, $s_q = -0.5$. Deviations of observer gains for figures a)–h) are defined in Table 1

Table 1. Deviations of observer gains (cf. Fig. 4)

a)	$0.9k_1$	$0.9k_2$	$0.9k_3$	e)	$0.9k_1$	$0.9k_2$	$1.1k_3$
b)	$1.1k_1$	$0.9k_2$	$0.9k_3$	f)	$1.1k_1$	$0.9k_2$	$1.1k_3$
c)	$0.9k_1$	$1.1k_2$	$0.9k_3$	g)	$0.9k_1$	$1.1k_2$	$1.1k_3$
d)	$1.1k_1$	$1.1k_2$	$0.9k_3$	h)	$1.1k_1$	$1.1k_2$	$1.1k_3$

3.3. ESTIMATION OF THE ROTOR POSITION ANGLE

For correct operation of the control system, the rotor position angle is required. The proposed structure of the state observer allows determining the stator flux and rotor current in the stator stationary reference frame. In DFIG, the rotor current is directly measured in the rotor reference frame. With the rotor current values in different reference frames, the rotor position can by calculated according to the formulas

$$\cos_{\varphi RS} = \frac{\hat{i}_{r\alpha S} i_{r\alpha R} + \hat{i}_{r\beta S} i_{r\beta R}}{\left|\bar{i}_R\right|} \quad \sin_{\varphi RS} = \frac{\hat{i}_{r\beta S} i_{r\alpha R} - \hat{i}_{r\alpha S} i_{r\beta R}}{\left|\bar{i}_R\right|} \tag{33}$$

where, subscripts αR, βR are the components of rotor current measured directly, and, accordingly, αS, βS are the components of the rotor current estimated in observer. Figure 1 shows a graphical interpretation of the above equations.

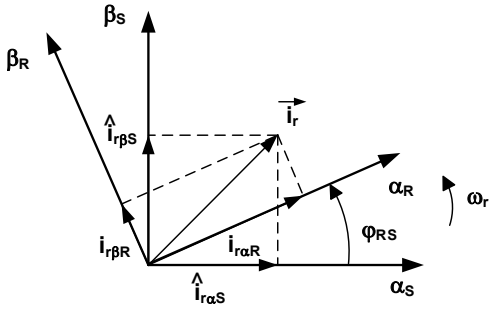

Fig. 5. The vector of rotor current in various reference frames

4. SIMULATION AND LABORATORY INVESTIGATIONS

To verify steady-state and dynamic performance of the proposed control system, simulation and laboratory tests were carried out. The performance of the proposed power control system with the state observer was evaluated using a software written in C++ language. The developed simulation software includes the generator model, power control system and state observer algorithms. The discrete nature of the control system and power converter was taken into account. The control cycle time for power converter and PWM algorithm ware implemented. The measurement procedure of rotor and stator currents and grid voltage was simulated in detail, taking influence of the sensors, sample and holds procedure. All the results presented are carried out on a 2 kW DFIG. Parameters of the generator expressed in per unit system used in the simulations are given in Table 2. The following basic values $U_b = 400$ V, $I_b = 9.526$ A, $\omega_b = 104.7$ rad/s have been assumed.

Table 2. The generator parameters in SI and per unit systems

Parameter	Value	
	SI	pu
Rotor resistance, R_r	2.53 Ω	0.0649
Stator resistance, R_s	2.97 Ω	0.0762
Rotor inductance, L_r	0.166 H	1.3378
Stator inductance, L_s	0.166 H	1.3378
Mutual inductance, L_m	0.158 H	1.2733
Stator/rotor ratio, n	–	1
Pair of poles, p	–	3

The scope of the simulation study includes an evaluation of the performance of the power control system and proposed state observer. Standard tests for doubly-fed generator were performed to demonstrate properties of the power control system. All observer parameters used in the algorithm have been changed by 5% with respect to the real generator parameters. Figure 6 shows the results of simulation for the DFIG system and state observer in response to the external driving torque changes. As a result of these changes, the rotational speed ω_r of the generator rotor increased from 0.8 to 1.3 of the synchronous speed. The power control system works properly in the whole range of changes in the rotational generator speed. The values of stator active power s_p and reactive power s_q were kept in reference levels. The error of speed estimation ω_{re} do not exceed 2% and oscillates around zero. The speed observer algorithm is stable.

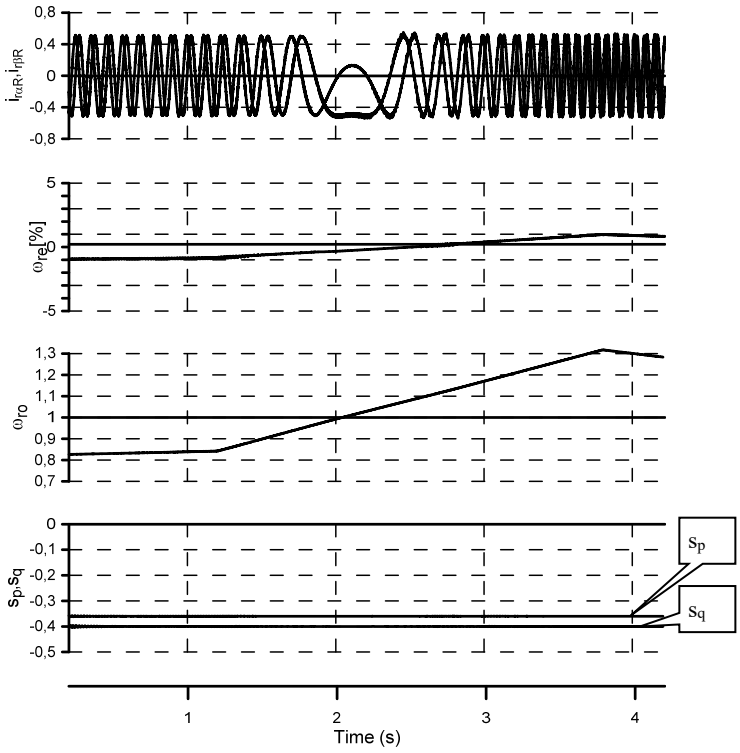

Fig. 6. Simulation of the generator response to an external driving torque steps

During the tests, the response to changes of reference values of the active s_p and reactive s_q power were examined to determine proper decoupling in both power control loops. Figure 7 shows the reaction of the power control system to the active power change from –0.35 pu to –0.2 pu at a constant reactive power equal to –0,4 pu and change of reactive power at a constant active power. No coupling in power control loops

was observed. Oscillations in power waveforms are the results of stator flux oscillations $|\Psi_s|$ and are slowly damped.

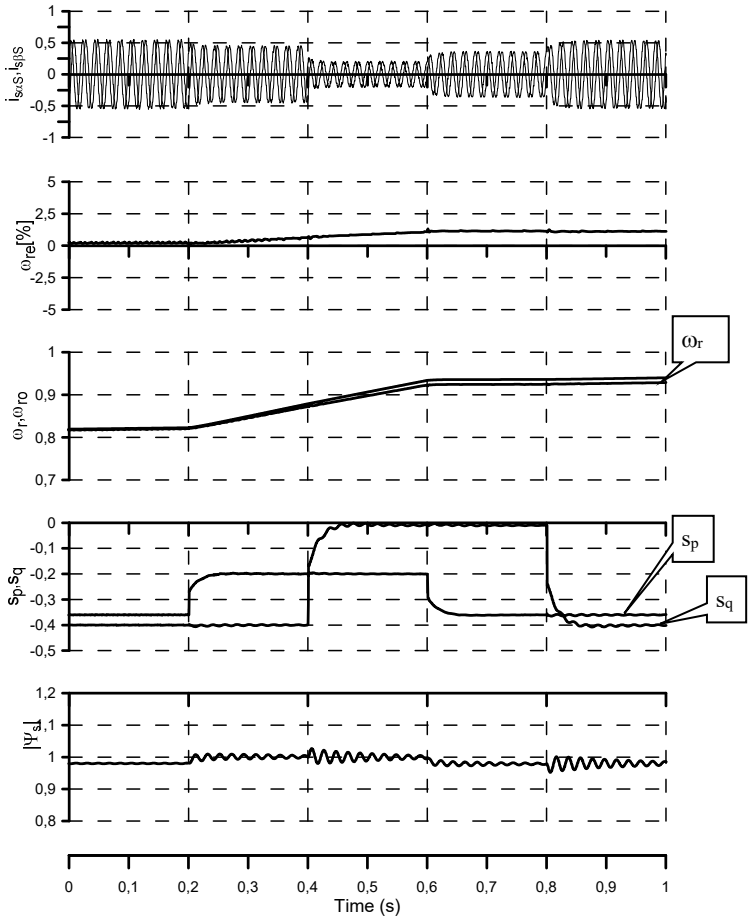

Fig. 7. Simulation of the response to active and reactive power steps

To confirm the simulation results, the laboratory tests were performed. The experimental verification was carried out on wound-rotor induction machine of the SUDf112-6 type mechanically coupled to the induction squirrel-cage motor. The incremental encoder with the resolution of 720 pulses was used as an auxiliary sensor to measure the actual rotor position and rotational speed. The stator of the generator was connected directly to the grid while the rotor was fed by a bi-directional power converter. All control algorithms were implemented on a digital control board including an ADSP-21363 digital signal processor with an Altera Cyclone II family FPGA chip. The control algorithm for the generator part of the laboratory setup was written in C language. The control cycle time was set at 150 μs. The whole experimental system was controlled from

a personal computer using a dedicated operator console. Figure 8 shows the response of the generator power control system to active power changes from –0.35 pu to –0.1 pu at a constant reactive power equal to –0,4 pu. Noticeable changes of estimated ω_{ro} and measured ω_r rotor speed were caused by generator load variations. The rotor speed error ω_{re} did not exceed 1%. Figure 9 shows the response of the generator control system to changes of the reactive power s_q from –0,6 pu to –0,1 pu at a constant active power s_p equal to –0,35 pu. The generator was working with lagging power factor in all the laboratory tests.

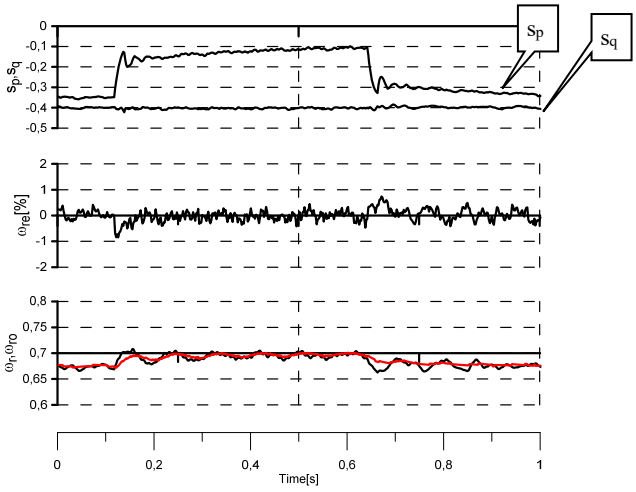

Fig. 8. The experimental results for stator active power s_p step changes, reactive power s_q is constant

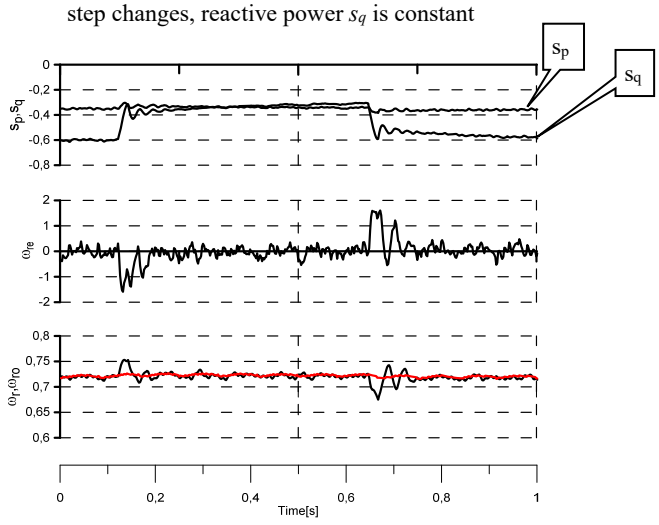

Fig. 9. The experimental results for stator reactive power s_q step changes, active power s_p is constant

Experimental results of the response of the power control system, in the case where generator speed slowly crosses a synchronous one, is presented in Fig. 10. During the test, both values of powers were equal to the reference value and the speed error oscillates around zero.

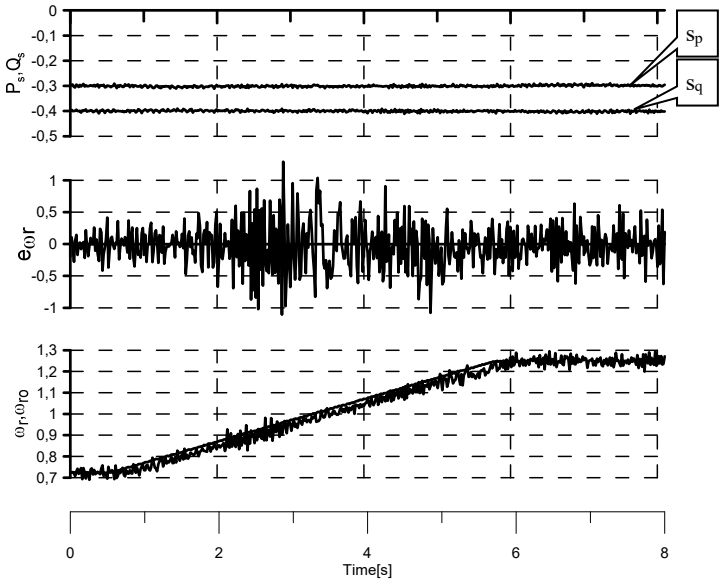

Fig. 10. Experimental result for crossing synchronous speed for a constant active and reactive power

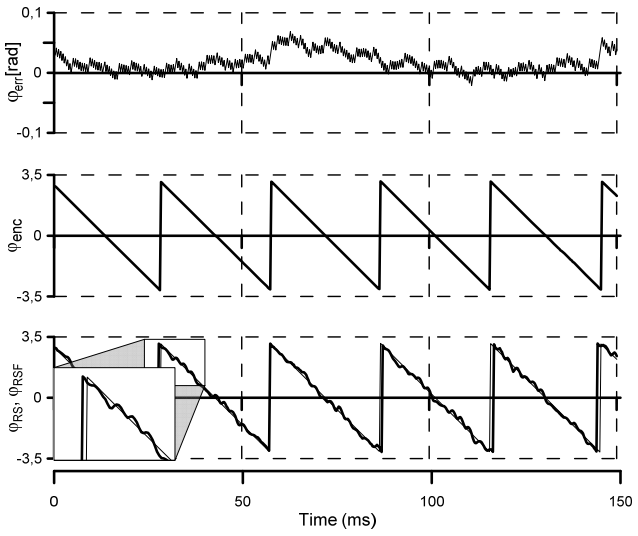

Fig. 11. The estimated and measured waveform of the rotor position angle

The measured φ_{enc} and estimated φ_{RS} rotor position angles for a steady-state operation are shown in Fig. 11. The steady-state operation of a rotational speed to 685 rev/min corresponds to a rotor angle change of 29.1 ms. The estimated rotor angle position φ_{RS} was deformed. In the power control algorithm, the filtered value of the angle φ_{RSF} was used. The error φ_{err} between measured and estimated rotor angles was about 2.5°.

5. CONCLUSION

The simulation and experimental verification of the operation of a nonlinear active and reactive power control system with a state observer have been presented. Simulations were carried out using a full-order model of the generator and the converter model. In the control algorithm, the discrete mode operation was taken into account. The active and reactive power step response was verified. The power regulation was independent in both control paths. In the assumed variation range of the rotor speed, the state observer was stable. The estimation error of rotor speed ω_{re} did not exceed 1%, where the stator flux error $|\boldsymbol{\psi}_s|_e$ was less than 1%. The angle of rotor position φ_{RSF} was determined with an error of 2.5°. The presented power control system with the speed observer algorithm is an interesting solution in relation to the classic field oriented method and direct power control method for DFIG.

REFERENCES

[1] MARQUES G.D., SOUSA D.M., *Sensorless direct slip position estimator of a DFIM based on the air gap pq vector-sensitivity study*, IEEE Trans. Ind. Electron., 2013, 60(6), 2442–2450.

[2] KARTHIKEYAN A., NAGAMANI C., CHAUDHURY A., RAY B., ILANGO G.S., *Implicit position and speed estimation algorithm without the flux computation for the rotor side control of doubly fed induction motor drive*, IET Electr. Power Appl., 2012, 6(4), 243–252.

[3] YANG S., AJJARAPU V., *A speed-adaptive reduced-order observer for sensorless vector control of doubly fed induction*, IEE Trans. En. Conv., 2010, 25(3), 891–900.

[4] YING L., CUI X., LIAO Q., TANG C.H., LE L.,CHEN Z., *Stator flux observation and speed estimation of a doubly fed induction generator*, International Conference on Power System Technology, Chongqinq, China, 22–26 October 2006, 1–6.

[5] IACCHETTI M.F., CARMELI M.S., CASTELLI DEZZA F., PERINI R., *A speed sensorless control based on a MRAS applied to a double fed induction machine drive*, Electr. Eng., 2010, 91(6), 337–345.

[6] CARDENAS R., PENA R., CLARE J., ASHER G., PROBOSTE J., *MRAS observers for sensorless control of doubly-fed induction generators*, IEEE Trans. Power Electron., 2008, 23(3), 1075–1084.

[7] GUZINSKI J., DIGUET M., KRZEMINSKI Z., LEWICKI A., ABU-RUB H., *Application of speed and load torque observers in high-speed train drive for diagnostic purpose*s, IEEE Trans. Ind. Electron., 2009, 56(1), 248–256.

[8] KRZEMIŃSKI Z., *Sensorless multiscalar control of double fed machine for wind power generators*, Proc. Power Conversion Conference, PCC, Osaka 2002, 334–339.

[9] BLECHARZ K., KRZEMINSKI Z., *A speed observer system for doubly fed induction generator*, Przegl. Elektr., 2012(11a), 34–37.